ACCOUNTS
of chemical research

High-Energy-Surface Engineered Metal Oxide Micro- and Nanocrystallites and Their Applications

QIN KUANG, XUE WANG, ZHIYUAN JIANG, ZHAOXIONG XIE,*
AND LANSUN ZHENG

State Key Laboratory of Physical Chemistry of Solid Surfaces and Department of Chemistry, College of Chemistry and Chemical Engineering, Xiamen University, Xiamen 361005, China

RECEIVED ON APRIL 3, 2013

CONSPECTUS

Because many physical and chemical processes occur at surfaces, surface atomic structure is a critical factor affecting the properties of materials. Due to the presence of high-density atomic steps and edges and abundant unsaturated coordination sites, micro- and nanocrystallites with high-energy surfaces usually exhibit greater reactivity than those with low-energy surfaces. However, high-energy crystal surfaces are usually lost during crystal growth as the total surface energy is minimized. Therefore, the selective exposure of high-energy facets at the surface of micro- and nanocrystallites is an important and challenging research topic. Metal oxides play important roles in surface-associated applications, including catalysis, gas sensing, luminescence, and antibiosis. The synthesis of metal oxide micro- and nanocrystallites with specific surfaces, particularly those with high surface energies, is more challenging than the synthesis of metal crystals due to the presence of strong metal–oxygen bonds and diverse crystal structures.

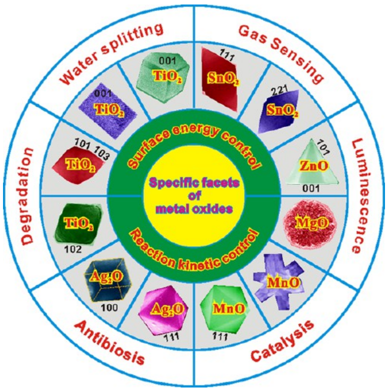

In this Account, we briefly summarize recent progress in the surface-structure-controlled synthesis of several typical metal oxide micro- and nanocrystallites, including wurtzite ZnO, anatase TiO$_2$, rutile SnO$_2$, and rocksalt-type metal oxides. We also discuss the improvement of surface properties, focusing on high-energy surfaces. Because of the huge quantity and diverse structure of metal oxides, this Account is not intended to be comprehensive. Instead, we discuss salient features of metal oxide micro- and nanocrystallites using examples primarily from our group.

We first discuss general strategies for tuning the surface structure of metal oxide micro- and nanocrystallites, presenting several typical examples. For each example, we describe the basic crystallographic characteristics as well as the thermodynamic (i.e., tuning surface energy) or kinetic (i.e., tuning reaction rates) strategies we have used to synthesize micro- and nanocrystallites with high surface energies. We discuss the structural features of the specific facets and analyze the basis for the enhanced performance of the metal oxide micro- and nanocrystallites in water splitting, the degradation of organic pollutants, gas sensing, catalysis, luminescence, and antibiosis. Finally, we note the future trends in high-energy-facet metal oxide micro- and nanocrystallite research. A comprehensive understanding of the properties of metal oxide micro- and nanocrystallites with high-energy crystal surfaces and related synthetic strategies will facilitate the rational design of functional nanomaterials with desired characteristics.

1. Introduction

Crystals with different types of exposed facets usually exhibit different physical and chemical properties; such anisotropy is one of the basic properties of crystals. Surface chemists have made great progress in elucidating the relationship between the surface structures of materials and their properties. However, our knowledge of surface science has primarily been obtained using bulk crystals in vacuum environments and thus cannot be directly applied to, for example, catalysis, which occurs under different conditions. The control of the surface structure of micro- and nanocrystallites may bridge this research–application gap.

While the specific surfaces of bulk crystals are readily exposed by mechanical cutting or grinding, the exposed

10.1021/ar400092x

surfaces of micro- and nanocrystallites are generated during crystal growth. However, chemically stable and less active crystal facets are usually exposed because exposure of the high-energy facets is energetically unfavorable and is therefore minimized during crystal growth. Because of the high density of atomic steps and edges and abundant unsaturated coordination sites, the reactivity of high-energy facets is usually greater than that of low-energy facets.[1] The exposure of high-energy facets is therefore important in both fundamental and application-based research. Theoretically, a high-energy surface can be fabricated either through the thermodynamic reduction of the surface energy via selective adsorption of capping agents on specific crystal faces or through control of the growth kinetics.[2−4] Despite extensive efforts over the past decade, the controlled synthesis or engineering of high-energy surfaces on micro- and nanocrystallites remains challenging.

Most of the advances in the engineering of surface structures have been achieved in face-centered cubic (fcc) noble-metal nanocrystals (e.g., Au, Pd, Pt, and their alloys),[3−6] which feature relatively weak and nondirectional metallic bonding. The strong metal−oxygen covalent bonding and the diverse crystal packing structure in metal oxides make surface engineering comparatively more difficult.[7] Nevertheless, progress has recently been made in the surface-controlled synthesis of metal oxide micro- and nanocrystallites to enhance their physicochemical properties.[8,9] To explore novel strategies for the synthesis of inorganic nanomaterials with unique surface structures and enhanced activities, a research account of surface-structure-engineered metal oxide micro- and nanocrystallites, particularly those with high-energy surfaces, appears to be timely.

In this Account, we begin with a brief discussion of general strategies for the fabrication of shaped micro- and nanocrystallites with exposed high-energy surfaces. This discussion is focused on our work and recent progress in surface structure engineering of metal oxide micro- and nanocrystallites and their improved surface properties, with particular emphasis on crystal facets of high surface energy. After a short discussion concerning the stability and activity of high-energy-surface engineered metal oxides, we conclude the Account with a discussion of challenging issues and future trends.

2. General Strategies for the Fabrication of Shaped Micro- and Nanocrystallites with Exposed Specific Faces

In crystallography, the equilibrium shape of a crystal is theoretically described by the Gibbs−Wulff theorem.[10] Under realistic conditions, however, the final shape of a crystal and the exposed facets are a result of the interplay between thermodynamics and kinetics. From a thermodynamic perspective, the selective adsorption of capping or stabilizing reagents (such as organic surfactants, polymers, small molecules, and ions) onto specific faces is an effective means of reducing surface energies and exposing crystal faces.[11−13] In this aspect, the results of theoretical and experimental surface science studies may provide guidelines for the rational design and fabrication of micro- and nanocrystallites with desired surface features. In addition, thermodynamic analysis has indicated that the supersaturation of growth species might determine the surface energy of exposed faces during crystal growth, which provides a general way for fabricating the specific high-energy surfaces on micro- and nanocrystallites.[14,15]

Kinetic control is another powerful method for tuning the shape and surface structure of micro- and nanocrystallites. In practice, crystals often grow under conditions that differ substantially from equilibrium conditions. Under nonequilibrium conditions, the shape of crystals is not unique and strongly depends on kinetic parameters such as the crystal growth rate during the nucleation and growth of crystals.[2,3,15−17] Compared with thermodynamic control of surface structure engineering, kinetic control involves a number of factors and is therefore more complicated, and the relationship between surface structure and kinetic factors remains unclear.

Thermodynamic and kinetic approaches to the synthesis of micro- and nanocrystallites with specific facets both represent bottom-up processes for crystal growth. In recent years, top-down strategies have also been applied to engineer the surface structure of micro- and nanocrystallites.[18,19] Directional chemical etching based on crystal anisotropy, which has been widely used in the semiconductor industry, has shown particular advantages in the fabrication of micro- and nanocrystallites with specific surface structures.

3. Case Studies

3.1. Metal Oxide Micro- And Nanocrystallites That Are Fully Enclosed by Polar Planes and Their Surface-Dependent Properties. The crystal structures of many ionic compounds, including those of metal oxides, can be simply described as a number of planes consisting of positively charged cations and negatively charged anions stacked in alternating fashion. These charged planes, such as wurtzite-type $\{0001\}$, rocksalt-type, and spinel-type $\{111\}$ planes, are known as polar planes (Figure 1a,d,g). Because the

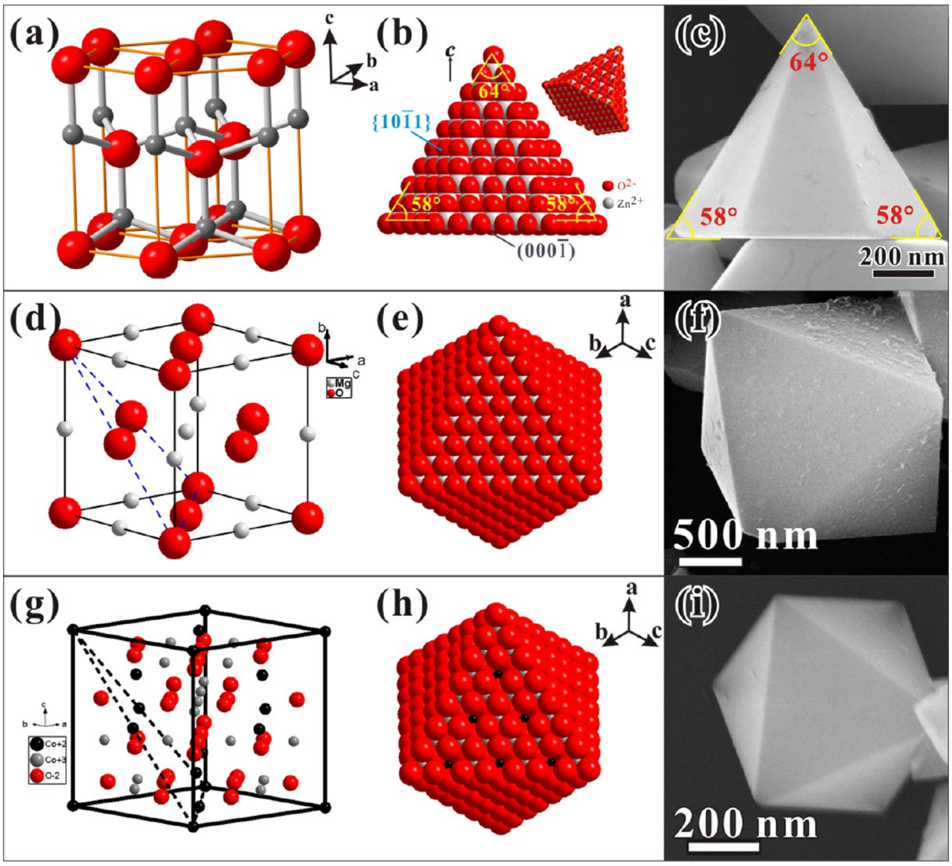

FIGURE 1. Crystal structures, ideal models, and SEM images of representative metal oxide crystals with polar facets: (a−c) wurtzite-type ZnO,[20] (d−f) rocksalt-type MgO,[21] and (g−i) spinel-type Co_3O_4.[21]

exposure of polar planes is energetically unfavorable due to their high surface energy, the surfaces of these ionic crystals are dominated by electrically neutral planes, for example, the $\{10\bar{1}0\}$ planes in wurtzite and the $\{100\}$ planes in rocksalt and spinel.

The surface energy of the polar planes can, in principle, be reduced by strong electrostatic interactions with oppositely charged additive species during crystal growth to achieve a structure with fully exposed polar planes. In wurtzite-type ZnO, the two groups of polar planes $\{0001\}$ and $\{10\bar{1}1\}$ form a hexagonal pyramidal structure (Figure 1b). As expected, pyramidal ZnO crystallites were generated via a thermolysis reaction of zinc acetate in molten salt or ionic liquids (Figure 1c).[20−22] Numerous metal oxide micro- and nanocrystallites that are fully enclosed by polar planes, such as $\{111\}$-exposed rocksalt-type MgO and MnO octahedra (Figure 1d−f), as well as spinel-type Co_3O_4 and $ZnFe_2O_4$ (Figure 1g−i), have been obtained via the aforementioned electrostatic interaction strategy.[21,23]

The polar planes of ionic metal oxides can also be controlled kinetically via elaborate tuning of reaction rates. For example, in the absence of any capping reagent, the shapes of cuprite-type Ag_2O particles can change from nonpolar $\{111\}$-faceted octahedra to polar $\{100\}$-faceted cubes when the concentrations of the starting precursor solutions are decreased 10-fold (Figure 2a).[24] Similarly, the kinetic route has been used to control the exposure of specific facets in another cuprite-type metal oxide, Cu_2O.[25] These examples fully demonstrate that kinetic control of the crystal growth rates enables tuning of the surface structures of metal oxide micro- and nanocrystallites. However, the effect of crystal growth kinetics on the morphology of micro- and nanocrystallites is unclear.

The unique structural features of polar surfaces often yield properties that differ from those of nonpolar surfaces. For example, because of their abundant active O^{2-} Lewis basic sites, O-terminated MgO octahedra possess high catalytic activity in Claisen−Schmidt condensation reactions.[26] The Zn^{2+}-terminated (0001) polar surface of ZnO crystallites exhibits very high gas-sensing sensitivity to ethanol and high photocatalytic activity in degradation processes.[27] Polar $\{100\}$-faceted Ag_2O cubes exhibit greater antibacterial

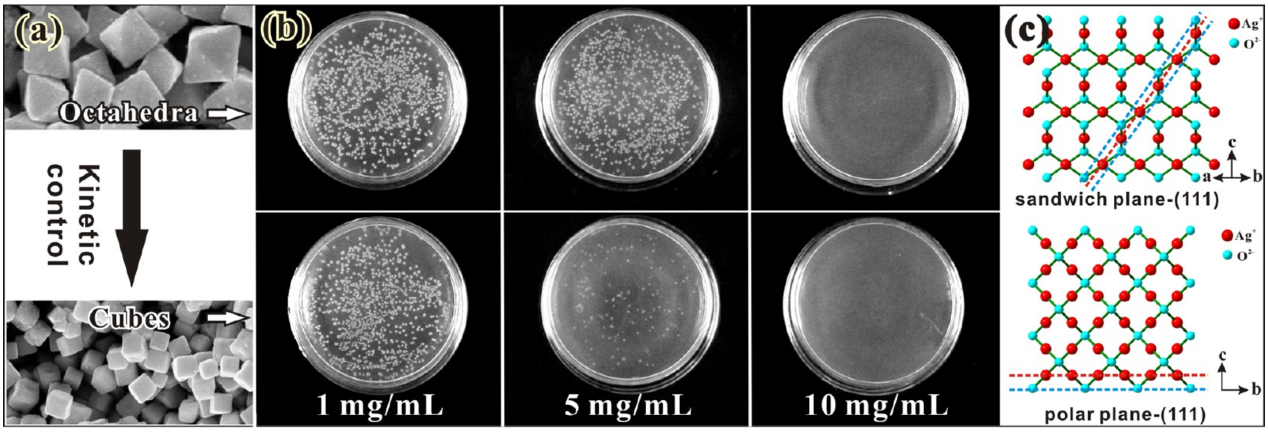

FIGURE 2. (a) Kinetically controlled shape evolution of cuprite-type Ag_2O from $\{111\}$-faceted octahedra to $\{100\}$-faceted cubes. (b) Comparison of the antibacterial activities (*E. coli*) of Ag_2O octahedra and cubes. (c) Illustration of the structural characteristics of the atoms in the $\{111\}$ and $\{100\}$ planes.[24]

activity against *Escherichia coli* than nonpolar $\{111\}$-faceted octahedra (Figure 2b) because the antibacterially active Ag^+ ions on the $\{100\}$ polar facets are more readily released than those on the sandwich-structured $\{111\}$ facets (Figure 2c).[24] Thus, the unique structural features associated with the polar surfaces of the metal oxide micro- and nanocrystallites confer numerous advantages that can be exploited in various applications.

3.2. Anatase-type TiO_2 Micro- and Nanocrystallites with Exposed High-Energy Facets and Their Enhanced Photocatalytic Properties. TiO_2 is a prototypical metal oxide because of its polytypic structures and wide variety of applications. The structural sensitivity of TiO_2 (including that of bulk-phase TiO_2 and its surfaces) in catalytic reactions has been widely investigated.[28−34] TiO_2 exhibits three main crystallographic phases: brookite, anatase, and rutile. The anatase phase has been studied extensively, particularly in catalysis, photocatalysis, and dye-sensitized solar cells. For anatase TiO_2, the average surface energies of different facets are 0.90 $J\ m^{-2}$ for the $\{001\}$ facet, 0.53 $J\ m^{-2}$ for the $\{100\}$ facet, and 0.44 $J\ m^{-2}$ for the $\{101\}$ facet.[32,33] The high-energy $\{001\}$ facet has a high density of unsaturated coordinated Ti atoms and active surface oxygen atoms with large Ti−O−Ti bond angles; it usually exhibits greater chemical activity than the other two low-energy facets.[32] However, anatase TiO_2 is thermodynamically apt to grow as a slightly truncated tetragonal bipyramid with eight exposed $\{101\}$ facets and two $\{001\}$ facets; the latter represent only 6% of the total facets.[32] To identify a suitable capping agent to stabilize the high-energy $\{001\}$ facets, first-principles calculations were applied. It was found that the adsorption of fluorine ions may markedly reduce the surface energy of the (001) surface to a level lower than that of $\{101\}$ surfaces.[8] According to this theoretical result, hydrofluoric acid (HF) was selected as the capping agent, and micrometer-sized truncated tetragonal pyramidal anatase TiO_2 with 47% $\{001\}$ facets exposed was first obtained by Lu et al. Soon after, we prepared TiO_2 nanosheets with a thickness of several nanometers, and the percentage of $\{001\}$ facets was increased to 89% (Figure 3a).[35] The highly exposed $\{001\}$ facets increased the photocatalytic activity of the TiO_2 nanosheets, compared with the benchmark photocatalyst (Degussa P25 TiO_2), in the degradation of methyl orange (MO) (Figure 3b). In addition to using HF as a capping agent, some precursors that contain fluoric ions, such as $TiOF_2$, can be directly converted to anatase TiO_2 with $\{001\}$ exposed facets due to the adsorption of fluoric ions on the surface (Figure 3c).[36]

The fluorine-ion capping strategy is not ideal because fluorine-containing capping reagents and their derivatives are toxic, corrosive, and harmful to human health. However, capped fluorine would significantly but inexplicably affect the photocatalytic activity.[37−39] Although fluorine can easily be removed from the surface of anatase single crystals via heat treatment or competitive adsorption of hydroxyl groups in NaOH solution, fluorine-free synthetic strategies are still desired. We subsequently determined that carbonate ions are a potential alternative to regulate the formation of $\{001\}$ facets of anatase TiO_2 because of the bidentate-chelating ability of carbonate ions.[40] Using carbonate ions, we synthesized highly truncated tetragonal pyramidal TiO_2 nanocrystals with a remarkable percentage (60%) of $\{001\}$ facets via the hydrothermal treatment of K-titanate nanofibers.[40,41] In addition to exposing $\{001\}$

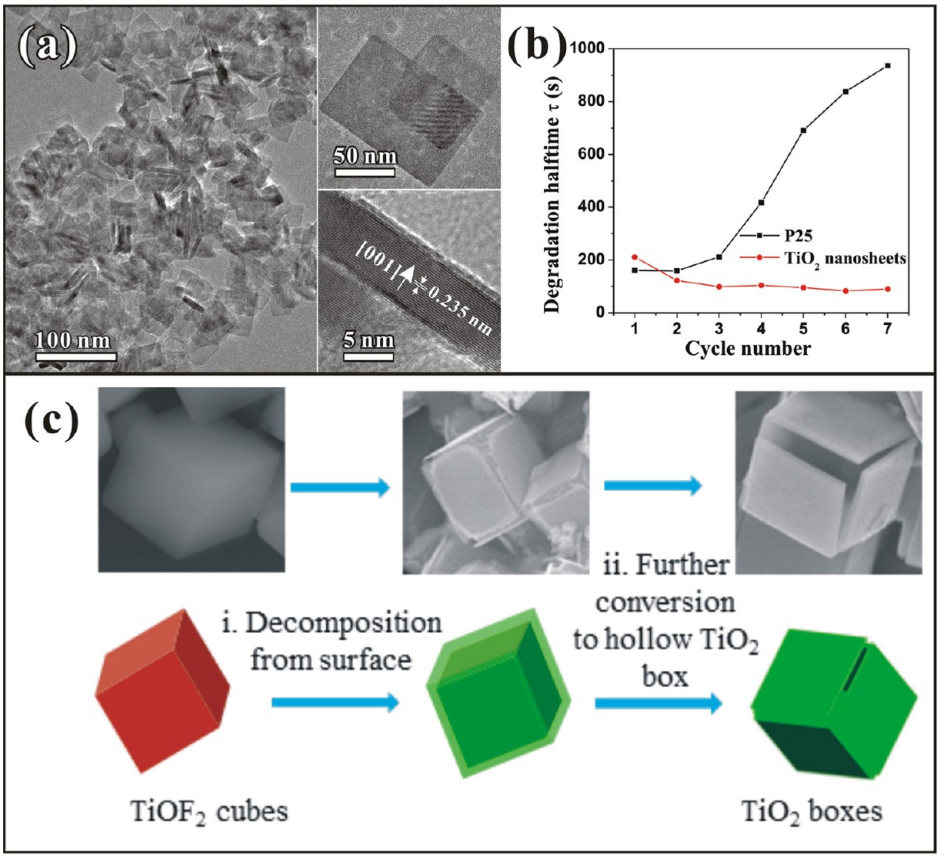

FIGURE 3. (a) TEM images and (b) evaluation of photocatalytic activity in MO degradation of TiO_2 nanosheets prepared using HF (47%) as a capping reagent. Reproduced with permission from ref 35. Copyright 2009 American Chemical Society. (c) Schematic of the synthesis of cubic TiO_2 boxes from the cubic $TiOF_2$ precursor. Reproduced with permission from ref 36. Copyright 2011 Royal Society of Chemistry.

facets, we also exposed {102} and {103} high-index facets with step structures on the surface of TiO_2 nanocrystals via similar carbonate-ion-assisted routes by adjusting the solvent composition.[42]

Different crystal facets can exhibit different physical/chemical behaviors. When the truncated tetragonal bipyramidal TiO_2 nanocrystals are used for the photoinduced deposition of Pt and PbO_2, the {101} facets provide the reductive sites, while the {001} facets provide the oxidative sites in the photoreaction due to differences in the preferred transfer directions of the photogenerated electrons and holes induced by the specific facets (Figure 4a).[30] As a consequence, after metal (e.g., Pt) nanoparticles are selectively deposited onto the {101} facets, the specific facet-induced spontaneous separation between photogenerated electrons and holes is likely to be strengthened, thereby enhancing the photocatalytic activities of TiO_2 nanocrystals. Consistent with this analysis, the photocatalytic efficiency of selective Pt-deposited TiO_2 nanocrystals in MO photodegradation is increased 2-fold compared with the efficiencies of nonselective Pt-deposited TiO_2 nanocrystals (Figure 4b). In addition, the efficiency in the photocatalytic reduction process (e.g., H_2 evolution from the splitting of water, Figure 4c) is increased 5-fold.[41] Specific facet-induced spontaneous separation between photogenerated electrons and holes has also been observed in numerous other metal oxide semiconductors, such as rutile-type TiO_2,[30] $BaTiO_3$,[43] $SrTiO_3$,[44] and $BiVO_4$.[45] Notably, the overall efficiency of semiconductor photocatalysts depends on the synergism between the photooxidation and photoreduction reactions in the photocatalytic process. Therefore, further exploration of the optimal ratio of oxidative and reductive facets for the controlled synthesis of faceted metal oxide photocatalysts is needed.[37,41]

3.3. Rutile-type SnO_2 Micro- And Nanocrystallites with Exposed High-Energy Facets and Their Enhanced Gas-Sensing and Catalytic Properties. Rutile SnO_2 is another functionally important metal oxide. The relative order of the average surface energies of the different facets is $2.280\ J\ m^{-2}$ for {221} > $2.209\ J\ m^{-2}$ for {111} > $1.648\ J\ m^{-2}$ for {100} > $1.554\ J\ m^{-2}$ for {101} > $1.401\ J\ m^{-2}$ for {110}.[46] The low-energy facets, {110}, {101}, and {100}, are usually

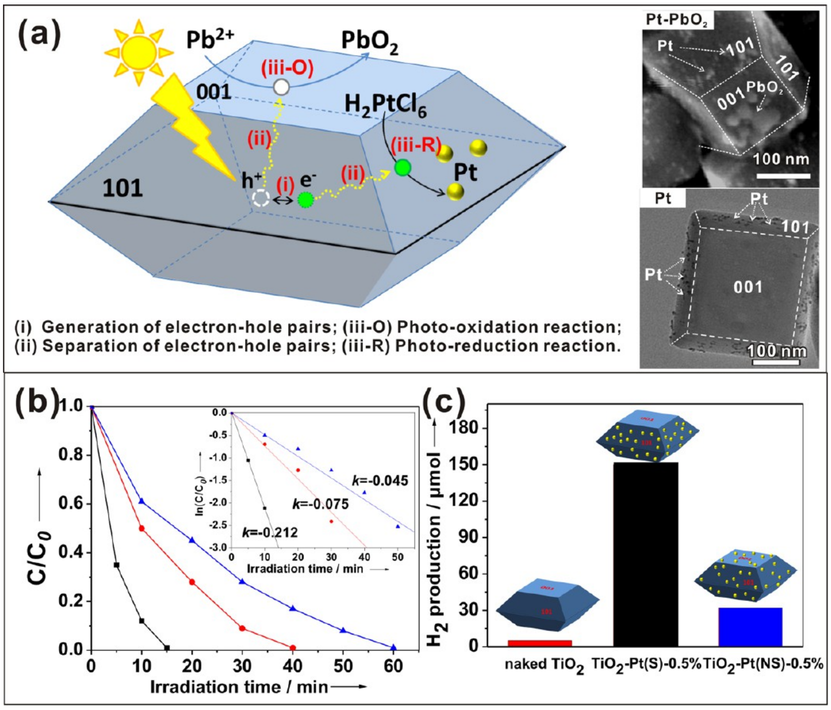

FIGURE 4. (a) Schematic illustration of facet-induced separation between photogenerated electrons and holes and the resulting facet-dependent photoreaction of anatase TiO_2 (upper right, deposition of PbO_2 nanoparticles on (001); lower right, deposition of Pt nanoparticles on (101). (b) Degradation curves of MO in the presence of the TiO_2 truncated tetragonal bipyramidal nanocrystals without deposition of Pt (naked TiO_2, ●), with selective deposition of Pt on {101} facets (TiO_2–Pt(S)-0.5%, ■), and with nonselective deposition of Pt (TiO_2–Pt(NS)-0.5%, ▲). The inset shows the corresponding kinetic rate curves (ln(C/C_0)–t). (c) The amount of H_2 evolved in the presence of the above three photocatalysts after irradiation for 6 h. Reproduced with permission from ref 41. Copyright 2013 Wiley-VCH.

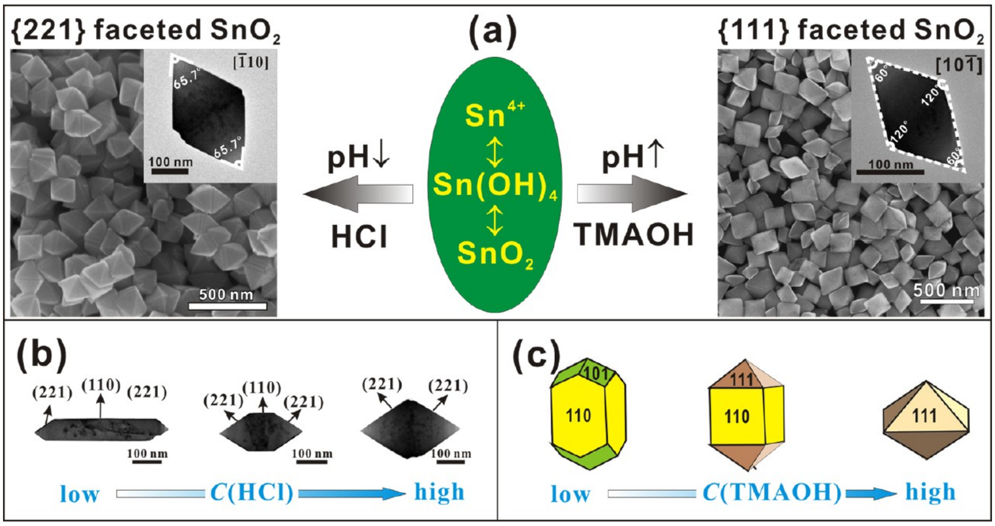

FIGURE 5. (a) Kinetic-controlled syntheses of {221}- or {111}-faceted SnO_2 octahedra via tuning of the hydrolysis–dehydration rates of Sn^{4+} ions with HCl or TMAOH. (b) Evolution of the morphology of SnO_2 nanocrystals with the concentration of HCl.[47] (c) Evolution of the morphology of SnO_2 nanocrystals with the concentration of TMAOH.[48]

dominant on the surface of rutile SnO_2 crystals. For the synthesis of SnO_2 nanoparticles, hydrolysis of Sn^{4+} ions in aqueous solution, in which Sn^{4+} is first hydrolyzed to $Sn(OH)_4$ and then dehydrated to SnO_2, is usually employed. Because $Sn(OH)_4$ is an amphoteric hydroxide, the pH value greatly affects the hydrolysis of Sn^{4+} ions and the dehydration of $Sn(OH)_4$ and thus affects the crystal growth kinetics of SnO_2 in aqueous solutions (Figure 5a). By increasing the

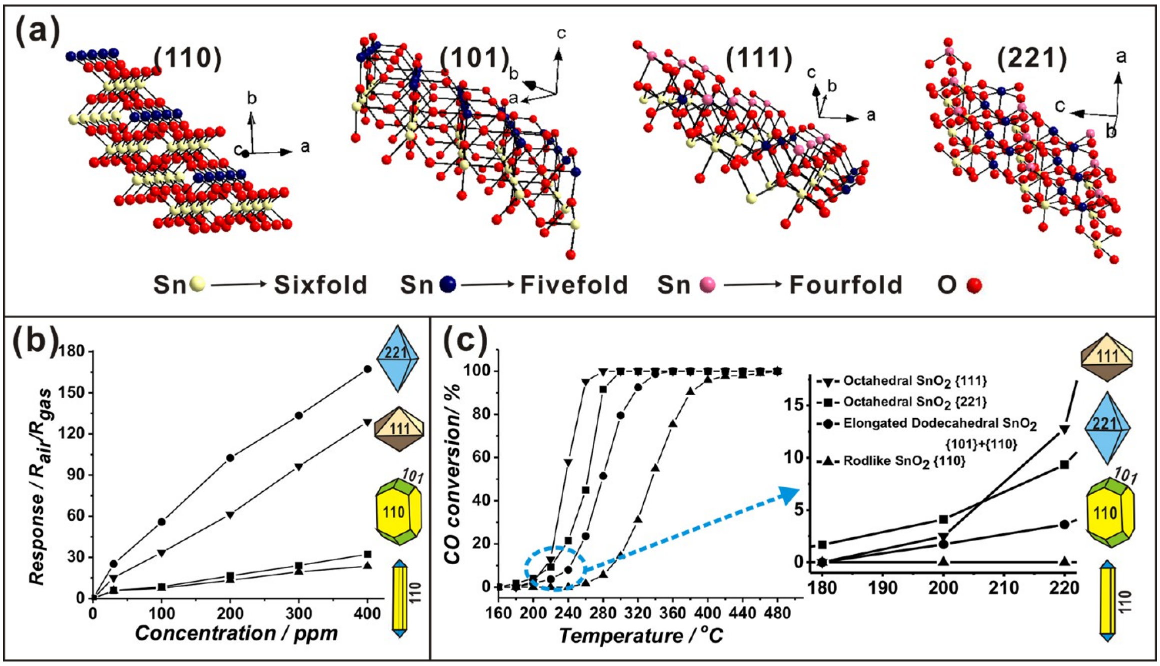

FIGURE 6. (a) Schematic models of the (110), (101), (111), and (221) facets. (b) Ethanol-concentration-dependent sensitivity curves, and (c) CO conversion curves of different faceted SnO_2 nanocrystals. The insets show the corresponding models of SnO_2 nanocrystals. Reproduced with permission from ref 48. Copyright 2012 Wiley-VCH.

acidity via the addition of hydrochloric acid (HCl), the formed SnO_2 particles evolve from low-energy {110}-faceted nanorods to {110}- and {221}-faceted elongated octahedra and high-energy {221}-faceted octahedra (Figure 5b).[47] The effect of changing basicity is similar to that of changing acidity. When the basicity of the reaction is increased via the addition of tetramethylammonium hydroxide (TMAOH), the shape evolves from {110}- and {101}-faceted elongated dodecahedra to high-energy {111}-faceted octahedra (Figure 5c).[48]

SnO_2 is one of the most commonly used gas-sensing materials. The gas-sensing response of metal-oxide semiconductors such as SnO_2 is directly correlated with their surface structure because the response involves an adsorption–desorption process of the detected gases on the semiconductor's surface. In contrast to the 6-fold-coordinated Sn atoms in the bulk, the coordinations of the Sn atoms on the surface are unsaturated (Figure 6a). For example, the rutile (110) surface contains rows of 6-fold-coordinated and 5-fold-coordinated Sn atoms, and all Sn atoms are 5-fold-coordinated on the (101) surface. For the high-energy (221) and (111) surfaces, five-coordinated and four-coordinated Sn atoms are observed. Surfaces such as (221) and (111), which contain unsaturated, low-coordinated metal atoms, are prone to adsorb more oxygen to form surface oxygen species (e.g., O_2^-, O^{2-}, or O^-), resulting in increased reactivity toward the reducing gas. We have consistently observed that the gas-sensing properties of the facets in rutile SnO_2 follow the order (221) > (111) ≫ (101) > (110) (Figure 6b).[47,48] The superior sensing performance of the {221} facets relative to the {111} facets may be due to the stepped structure, which favors the adsorption of the ionized oxygen species. Elucidation of the relationship between the surface structure and the gas-sensing behavior will provide deep insights into the nature of the gas-sensing mechanism of semiconductors at an atomic level.[49] As such, we believe that our research represents the first step toward atomic surface-structure control of gas-sensing activity. Interestingly, the activity order of SnO_2 facets in the catalytic oxidation of CO is not consistent with that in gas sensing. In CO oxidation, the temperature for 100% conversion of CO on the {221} facets is higher than that on the {111} facets, even though the starting conversion temperature on the {221} facets is lower (Figure 6c).[48] The abnormal catalytic performance on the {221} facets can be attributed to the more open structure of the {221} facets, which facilitates poisoning of the catalytically active sites. Thus, both the activity and stability of the high-energy facets should be given full consideration when designing for surface exposure.

3.4. Selective Chemical Etching: Top-down Engineering of Surface Structures of Metal-Oxide Micro- and Nanocrystallites. We have shown that well-defined shapes of

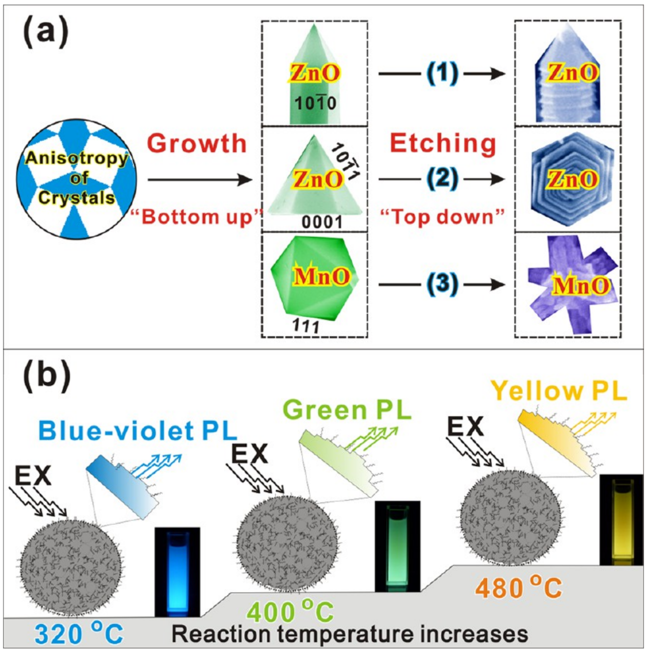

FIGURE 7. (a) Schematic illustration of the surface structure of metal oxide micro- and nanocrystallites fabricated by bottom-up growth routes and top-down etching routes; the illustration is based on the anisotropy of crystals: (1) rod-like ZnO to pagoda-like ZnO;[50] (2) pyramidal ZnO to spiral ZnO;[51] (3) octahedral MnO to six-horn-like MnO.[52] (b) Tunable PL of MgO nanocrystal clusters fabricated in the presence of OA under different reaction temperatures. Reproduced with permission from ref 53. Copyright 2011 Royal Society of Chemistry.

metal oxide micro- and nanocrystallites with exposed specific facets can be generated in a bottom-up manner via thermodynamic or kinetic control during crystal growth (Figure 7a). Due to the anisotropic properties of crystals, selective chemical etching can occur in different facets to produce micro- and nanocrystallites with special surface structures. For example, the differing reactivities of oleic acid (OA) with metal ions of different crystal facets enabled the preparation of pagoda-like microcrystallites (Figure 7a-1) and spiral micropyramids (Figure 7a-2) of ZnO with high-energy polar surfaces as well as six-horn-like MnO nanocrystals (Figure 7a-3).[50−52] Furthermore, the etching process begins at defective sites, suggesting that selective chemical etching may provide a unique tool for investigating the growth mechanism of nanocrystals. Some intrinsic structural features concealed in ZnO micro- and nanocrystallites, such as the twinned interface and the screw dislocation, have been vividly revealed via the etching technique.[50,51]

The properties of etched micro- and nanocrystallites may vary with the altered surface structures. For example, spiral ZnO pyramids exhibit greater gas-sensing ability than unetched ZnO pyramids due to both the newly exposed Zn^{2+}-terminated $(10\bar{1}1)$ planes and the increased surface area.[51] Notably, etching may produce abundant surface defects (typically as low-coordinated oxygen ions) on metal oxide micro- and nanocrystallites, and such newly generated surface defects may influence the properties of the metal oxides. Typically, intense, wavelength-tunable photoluminescence (PL) from the blue-violet region to the yellow region can be observed from single-crystal-like MgO nanocrystal clusters fabricated in the presence of OA at different temperatures (Figure 7b).[53] Such tunability is attributed to the synergistic effects that result from the coordinated sites, the capping OA, and the carbonate species on the surface of MgO nanocrystals. Reports based on top-down selective etching remain limited, likely due to the difficulties in selecting an appropriate etchant. However, the accuracy and the efficiency of selective chemical etching in the fabrication of specific surfaces have been demonstrated. These methodological advantages encourage the exploration and improvement of selective etching applications for the surface engineering of metal oxide micro- and nanocrystallites with specific surfaces, including high-energy facets.

4. Other Key Issues for Engineering High-Energy Surfaces of Metal-Oxide Micro- and Nanocrystallites and Their Applications

We have discussed the engineering of high-energy surfaces of metal-oxide micro- and nanocrystallites via thermodynamic control, kinetic control, and selective chemical etching. Despite great progress in controlling high-energy facets, key problems remain unresolved. We usually discuss micro- and nanocrystallites with ideal and clean crystal surfaces, which are never the case for shaped micro- and nanocrystallites, particularly those prepared via the capping-agent routes, in which the capping agent adsorbs and stabilizes high-surface-energy facets. Thus, caution is needed in drawing conclusions about the crystal facet effect of micro- and nanocrystallites to avoid obtaining contradictory results.[37−39] To avoid effects not related to the crystal facet itself, removal of the stabilizing agents, usually via calcination or exchange with weaker-binding adsorbates, may be required. After the capping reagents have been removed from the surfaces of the nanocrystals, the unprotected nanocrystals, particularly the high-energy facets, may undergo surface reconstruction. This surface reconstruction may also lead to unexpected changes in the properties of the metal-oxide micro- and nanocrystallites. In addition to the real surface structure of exposed crystal facets, the stability of high-energy facets should also be considered.

High-energy facets, when formed, are thermally stable to some extent. For example, the high-index (520) facet of Pt nanocrystals is thermally stable up to 800 °C under vacuum.[1] However, edge and vertex atoms with much lower coordination numbers and greater chemical activity inevitably exist on the surface of crystallites. The decrease in crystallite size increases the surface area of the specific high-energy surface but greatly decreases structural stability due to the presence of abundant edge and vertex atoms on the crystallites. Therefore, size control must be considered in practical applications of faceted nanocrystallites and is critical for balancing the activity and stability of the specific high-energy facets.

5. Concluding Remarks

In this Account, we have briefly summarized our efforts in engineering surface structures (with emphasis on high-energy facets) of metal oxide micro- and nanocrystallites to enhance their performance in surface-related applications. We have used well-characterized examples to clarify some intrinsic thermodynamic and kinetic issues in the surface-controlled synthesis of metal oxide micro- and nanocrystallites. As expected, metal oxide micro- and nanocrystallites that are enclosed by unusual high-energy facets exhibit enhanced performance in photodegradation, water splitting, gas sensing, catalysis, luminescence, and antibiosis.

Our understanding of the synthesis of micro- and nanocrystallites with specific facets and the relationship between activity and surface structure is still limited. We propose the following future research directions for metal oxides with high-energy facets. (1) The growth mechanism of high-energy facets, particularly high-index facets with steps and kinks, should be further investigated to provide guidelines for the controlled synthesis of metal oxide micro- and nanocrystallites with specific facets. The knowledge acquired from surface science studies and theoretical investigations will be critical for this aspect. (2) Intrinsic factors related to the kinetically controlled synthesis of metal oxide micro- and nanocrystallites with specific facets must be elucidated. The development of in situ spectroscopic and microscopic techniques is important for such kinetic studies. (3) The structural stability, in addition to the activity, of high-energy facets should be properly considered. Structural stability is important for nanosized crystallites used in different fields because it affects the actual performance of these materials over the long-term and in complex environments. (4) With respect to the synergy effect, the construction of epitaxial heterojunction and monatomic-layer-level modification of high-energy crystal surfaces may represent another important direction toward enhancing the performance of metal oxide micro- and nanocrystallites with high-energy surfaces. Overall, in-depth and comprehensive studies of the surface-structure engineering of metal oxides, particularly those with exposed high-energy facets, will lead to the rational design and synthesis of functional nanomaterials with exceptional properties.

We are grateful to our collaborators and other workers, as cited, for their invaluable contributions to this research field. We particularly appreciate selfless assistance from Prof. L. Chen at Indiana University Bloomington with polishing our manuscript. This work was supported by the National Basic Research Program of China (Grants 2011CBA00508 and 2013CB933901), the National Natural Science Foundation of China (Grants 21131005, 21333008, 21073145, and 21171142), and the program for New Century Excellent Talents in University (Grant NCET-11-0294).

BIOGRAPHICAL INFORMATION

Qin Kuang received his B.S. (2001) in Chemistry and Ph.D. (2008) in Chemistry from Xiamen University, China, with Prof. Lansun Zheng. He is currently an Associate Professor of Chemistry at Xiamen University. His current research is focused on surface/interface engineering of inorganic functional nanomaterials and their applications in the energy and environmental fields.

Xue Wang received her B.S. (2009) in Chemistry from Liaoning University, China. She is now pursuing her Ph.D. degree in physical chemistry at Xiamen University with Prof. Zhaoxiong Xie. She is currently working on the shape-controlled synthesis of metal oxide nanocrystals for environmental and energy-related applications.

Zhiyuan Jiang received his B.S. (1990) in Chemistry from Peking University and his M.S. (1995) and Ph.D. (2002) in Inorganic Chemistry from Xiamen University, China. He is currently a Professor of Chemistry at Xiamen University. His current research is focused on inorganic nanomaterials, with particular focus on solar cell applications.

Zhaoxiong Xie received his B.S. (1987) in Chemistry and his M.S. (1990) and Ph.D. (1995) in Physical Chemistry from Xiamen University, China. Since 2002, he has held the position of Professor of Physical Chemistry at Xiamen University. His current research is focused on the surface/interface chemistry of functional nanocrystals and self-assemblies of molecules via weak interactions on solid surfaces.

Lansun Zheng received his B.S. (1982) in Chemistry from Xiamen University, China, and his Ph.D. (1986) in Physical Chemistry from Rice University with Professor Richard E. Smalley. He is a Professor of Chemistry at Xiamen University. His current research is focused on the study of clusters, coordination compounds, and nanomaterials.

FOOTNOTES

*Corresponding author. E-mail: zxxie@xmu.edu.cn. Tel: 86 592 2180627.

The authors declare no competing financial interest.

REFERENCES

1 Tian, N.; Zhou, Z. Y.; Sun, S. G.; Ding, Y.; Wang, Z. L. Synthesis of Tetrahexahedral Platinum Nanocrystals with High-Index Facets and High Electro-Oxidation Activity. *Science* **2007**, *316*, 732–735.

2 Kwon, S. G.; Hyeon, T. Colloidal Chemical Synthesis and Formation Kinetics of Uniformly Sized Nanocrystals of Metals, Oxides, and Chalcogenides. *Acc. Chem. Res.* **2008**, *41*, 1696–1709.

3 Barnard, A. S. Direct Comparison of Kinetic and Thermodynamic Influences on Gold Nanomorphology. *Acc. Chem. Res.* **2012**, *45*, 1688–1697.

4 Xia, Y. N.; Xiong, Y. J.; Lim, B.; Skrabalak, S. E. Shape-Controlled Synthesis of Metal Nanocrystals: Simple Chemistry Meets Complex Physics? *Angew. Chem., Int. Ed.* **2009**, *48*, 60–103.

5 Zhou, Z. Y.; Tian, N.; Li, J. T.; Broadwell, I.; Sun, S. G. Nanomaterials of High Surface Energy with Exceptional Properties in Catalysis and Energy Storage. *Chem. Soc. Rev.* **2011**, *40*, 4167–4185.

6 Quan, Z. W.; Wang, Y. X.; Fang, J. Y. High-Index Faceted Noble Metal Nanocrystals. *Acc. Chem. Res.* **2013**, *46*, 191–202.

7 Zhou, K. B.; Li, Y. D. Catalysis Based on Nanocrystals with Well-Defined Facets. *Angew. Chem., Int. Ed.* **2012**, *51*, 602–613.

8 Yang, H. G.; Sun, C. H.; Qiao, S. Z.; Zou, J.; Liu, G.; Smith, S. C.; Cheng, H. M.; Lu, G. Q. Anatase TiO_2 Single Crystals with a Large Percentage of Reactive Facets. *Nature* **2008**, *453*, 638–U4.

9 Xie, X. W.; Li, Y.; Liu, Z. Q.; Haruta, M.; Shen, W. J. Low-Temperature Oxidation of CO Catalysed by Co_3O_4 Nanorods. *Nature* **2009**, *458*, 746–749.

10 Dobrushin, R. L.; Kotecky, R.; Shlosman, S. *Wulff Construction: A Global Shape from Local Interactions*; American Mathematical Society: Providence, RI, 1992.

11 Tao, A. R.; Habas, S.; Yang, P. D. Shape Control of Colloidal Metal Nanocrystals. *Small* **2008**, *4*, 310–325.

12 Xiong, Y. J.; Xia, Y. N. Shape-Controlled Synthesis of Metal Nanostructures: The Case of Palladium. *Adv. Mater.* **2007**, *19*, 3385–3391.

13 Chen, M.; Wu, B. H.; Yang, J.; Zheng, N. F. Small Adsorbate-Assisted Shape Control of Pd and Pt Nanocrystals. *Adv. Mater.* **2012**, *24*, 862–879.

14 Lin, H. X.; Lei, Z. C.; Jiang, Z. Y.; Hou, C. P.; Liu, D. Y.; Xu, M. M.; Tian, Z. Q.; Xie, Z. X. Supersaturation-Dependent Surface Structure Evolution: From Ionic, Molecular to Metallic Micro/Nanocrystals. *J. Am. Chem. Soc.* **2013**, *135*, 9311–9314.

15 Hu, W. B.; Li, L. P.; Tong, W. M.; Li, G. S. Supersaturated Spontaneous Nucleation to TiO_2 Microspheres: Synthesis and Giant Dielectric Performance. *Chem. Commun.* **2010**, *46*, 3113–3115.

16 Kang, L. T.; Fu, H. B.; Cao, X. Q.; Shi, Q. A.; Yao, J. N. Controlled Morphogenesis of Organic Polyhedral Nanocrystals from Cubes, Cubooctahedrons, to Octahedrons by Manipulating the Growth Kinetics. *J. Am. Chem. Soc.* **2011**, *133*, 1895–1901.

17 Langille, M. R.; Personick, M. L.; Zhang, J.; Mirkin, C. A. Defining Rules for the Shape Evolution of Gold Nanoparticles. *J. Am. Chem. Soc.* **2012**, *134*, 14542–14554.

18 Radjenovic, B.; Radmilovic-Raduenovic, M. Top-down Nanotechnologies in Surface Modification of Materials. *Cent. Eur. J. Phys.* **2011**, *9*, 265–275.

19 Hobbs, R. G.; Petkov, N.; Holmes, J. D. Semiconductor Nanowire Fabrication by Bottom-Up and Top-Down Paradigms. *Chem. Mater.* **2012**, *24*, 1975–1991.

20 Zhou, X.; Xie, Z. X.; Jiang, Z. Y.; Kuang, Q.; Zhang, S. H.; Xu, T.; Huang, R. B.; Zheng, L. S. Formation of ZnO Hexagonal Micro-Pyramids: A Successful Control of the Exposed Polar Surfaces with the Assistance Of an Ionic Liquid. *Chem. Commun.* **2005**, 5572–5574.

21 Xu, T.; Zhou, X.; Jiang, Z. Y.; Kuang, Q.; Xie, Z. X.; Zheng, L. S. Syntheses of Nano/Submicrostructured Metal Oxides with All Polar Surfaces Exposed via a Molten Salt Route. *Cryst. Growth Des.* **2009**, *9*, 192–196.

22 Zhou, X.; Kuang, Q.; Jiang, Z. Y.; Xie, Z. X.; Xu, T.; Huang, R. B.; Zheng, L. S. The Origin of Green Emission of ZnO Microcrystallites: Surface-Dependent Light Emission Studied by Cathodoluminescence. *J. Phys. Chem. C* **2007**, *111*, 12091–12093.

23 Xie, S. F.; Zhou, X.; Han, X. G.; Kuang, Q.; Jin, M. S.; Jiang, Y. Q.; Xie, Z. X.; Zheng, L. S. Supercrystals from Crystallization of Octahedral MnO Nanocrystals. *J. Phys. Chem. C* **2009**, *113*, 19107–19111.

24 Wang, X.; Wu, H. F.; Kuang, Q.; Huang, R. B.; Xie, Z. X.; Zheng, L. S. Shape-Dependent Antibacterial Activities of Ag_2O Polyhedral Particles. *Langmuir* **2010**, *26*, 2774–2778.

25 Wang, X.; Liu, C.; Zheng, B. J.; Jiang, Y. Q.; Zhang, L.; Xie, Z. X.; Zheng, L. S. Controlled Synthesis of Concave Cu_2O Microcrystals Enclosed by {hhl} High-Index Facets and Enhanced Catalytic Activity. *J. Mater. Chem. A* **2013**, *1*, 282–287.

26 Jiang, Z. Y.; Kuang, Q.; Xie, Z. X.; Zheng, L. S. Syntheses and Properties of Micro/Nanostructured Crystallites with High-Energy Surfaces. *Adv. Funct. Mater.* **2010**, *20*, 3634–3645.

27 Han, X. G.; He, H. Z.; Kuang, Q.; Zhou, X.; Zhang, X. H.; Xu, T.; Xie, Z. X.; Zheng, L. S. Controlling Morphologies and Tuning the Related Properties of Nano/Microstructured ZnO Crystallites. *J. Phys. Chem. C* **2009**, *113*, 584–589.

28 Hotsenpiller, P. A. M.; Bolt, J. D.; Farneth, W. E.; Lowekamp, J. B.; Rohrer, G. S. Orientation Dependence of Photochemical Reactions on TiO_2 Surfaces. *J. Phys. Chem. B* **1998**, *102*, 3216–3226.

29 Wilson, J. N.; Idriss, H. Structure Sensitivity and Photocatalytic Reactions of Semiconductors. Effect of the Last Layer Atomic Arrangement. *J. Am. Chem. Soc.* **2002**, *124*, 11284–11285.

30 Ohno, T.; Sarukawa, K.; Matsumura, M. Crystal Faces of Rutile and Anatase TiO_2 Particles and Their Roles in Photocatalytic Reactions. *New J. Chem.* **2002**, *26*, 1167–1170.

31 Lowekamp, J. B.; Rohrer, G. S.; Hotsenpiller, P. A. M.; Bolt, J. D.; Farneth, W. E. Anisotropic Photochemical Reactivity of Bulk TiO_2 Crystals. *J. Phys. Chem. B* **1998**, *102*, 7323–7327.

32 Lazzeri, M.; Vittadini, A.; Selloni, A. Structure and Energetics of Stoichiometric TiO_2 Anatase Surfaces. *Phys. Rev. B* **2001**, *63*, No. 155409.

33 Diebold, U. The Surface Science of Titanium Dioxide. *Surf. Sci. Rep.* **2003**, *48*, 53–229.

34 Lin, H. F.; Li, L. P.; Zaho, M. L.; Huang, X. S.; Chen, X. M.; Li, G. S.; Yu, R. C. Synthesis of High-Quality Brookite TiO2 Single-Crystalline Nanosheets with Specific Facets Exposed: Tuning Catalysts from Inert to Highly Reactive. *J. Am. Chem. Soc.* **2012**, *134*, 8328–8331.

35 Han, X. G.; Kuang, Q.; Jin, M. S.; Xie, Z. X.; Zheng, L. S. Synthesis of Titania Nanosheets with a High Percentage of Exposed (001) Facets and Related Photocatalytic Properties. *J. Am. Chem. Soc.* **2009**, *131*, 3152–3153.

36 Xie, S. F.; Han, X. G.; Kuang, Q.; Fu, J.; Zhang, L.; Xie, Z. X.; Zheng, L. S. Solid State Precursor Strategy for Synthesizing Hollow TiO_2 Boxes with a High Percentage of Reactive {001} Facets Exposed. *Chem. Commun.* **2011**, *47*, 6722–6724.

37 Zheng, Z. K.; Huang, B. B.; Lu, J. B.; Qin, X. Y.; Zhang, X. Y.; Dai, Y. Hierarchical TiO_2 Microspheres: Synergetic Effect of {001} and {101} Facets for Enhanced Photocatalytic Activity. *Chem.—Eur. J* **2011**, *17*, 15032–15038.

38 Pan, J.; Liu, G.; Lu, G. M.; Cheng, H. M. On the True Photoreactivity Order of {001}, {010}, and {101} Facets of Anatase TiO_2 Crystals. *Angew. Chem., Int. Ed.* **2011**, *50*, 2133–2137.

39 Luan, Y. B.; Jing, L. Q.; Xie, Y.; Sun, X. J.; Feng, Y. J.; Fu, X. G. Exceptional Photocatalytic Activity of 001-Facet-Exposed TiO_2 Mainly Depending on Enhanced Adsorbed Oxygen by Residual Hydrogen Fluoride. *ACS Catal.* **2013**, *3*, 1378–1385.

40 Han, X. G.; Wang, X.; Xie, S. F.; Kuang, Q.; Ouyang, J. J.; Xie, Z. X.; Zheng, L. S. Carbonate Ions-Assisted Syntheses of Anatase TiO_2 Nanoparticles Exposed with High Energy (001) Facets. *RSC Adv.* **2012**, *2*, 3251–3253.

41 Liu, C.; Han, X. G.; Xie, S. F.; Kuang, Q.; Wang, X.; Jin, M. S.; Xie, Z. X.; Zheng, L. S. Enhancing the Photocatalytic Activity of Anatase TiO_2 by Improving the Specific Facet-Induced Spontaneous Separation of Photogenerated Electrons and Holes. *Chem.—Asian J.* **2013**, *8*, 282–289.

42 Han, X. G.; Zheng, B. J.; Ouyang, J. J.; Wang, X.; Kuang, Q.; Jiang, Y. Q.; Xie, Z. X.; Zheng, L. S. Control of Anatase TiO_2 Nanocrystals with a Series of High-Energy Crystal Facets via a Fuorine-Free Strategy. *Chem—Asian J.* **2012**, *7*, 2538–2542.

43 Giocondi, J. L.; Rohrer, G. S. Spatial Separation of Photochemical Oxidation and Reduction Reactions on the Surface of Ferroelectric $BaTiO_3$. *J. Phys. Chem. B* **2001**, *105*, 8275–8277.

44 Giocondi, J. L.; Salvador, P. A.; Rohrer, G. S. The Origin of Photochemical Anisotropy in $SrTiO_3$. *Top. Catal.* **2007**, *44*, 529–533.

45 Li, R. G.; Zhang, F. X.; Wang, D. G.; Yang, J. X.; Li, M. R.; Zhu, J.; Zhou, X.; Han, H. X.; Li, C. Spatial Separation of Photogenerated Electrons and Holes among {010} and {110} Crystal Facets of $BiVO_4$. *Nat. Commun.* **2013**, *4*, No. 1432.

46 Batzill, M.; Katsiev, K.; Burst, J. M.; Diebold, U.; Chaka, A. M.; Delley, B. Gas-Phase-Dependent Properties of SnO_2 (110), (100), and (101) Single-Crystal Surfaces: Structure, Composition, and Electronic Properties. *Phys. Rev. B* **2005**, *72*, No. 165414.

47 Han, X. G.; Jin, M. S.; Xie, S. F.; Kuang, Q.; Jiang, Z. Y.; Jiang, Y. Q.; Xie, Z. X.; Zheng, L. S. Synthesis of Tin Dioxide Octahedral Nanoparticles with Exposed High-Energy {221} Facets and Enhanced Gas-Sensing Properties. *Angew. Chem., Int. Ed.* **2009**, *48*, 9180–9183.

48 Wang, X.; Han, X. G.; Xie, S. F.; Kuang, Q.; Jiang, Y. Q.; Zhang, S. B.; Mu, X. L.; Chen, G. X.; Xie, Z. X.; Zheng, L. S. Controlled Synthesis and Enhanced Catalytic and Gas-Sensing Properties of Tin Dioxide Nanoparticles with Exposed High-Energy Facets. *Chem.—Eur. J.* **2012**, *18*, 2283–2289.

49 Gurlo, A. Nanosensors: Towards Morphological Control of Gas Sensing Activity. SnO_2, In_2O_3, ZnO and WO_3 Case Studies. *Nanoscale* **2011**, *3*, 154–165.

50 Han, X. G.; Jiang, Y. Q.; Xie, S. F.; Kuang, Q.; Zhou, X.; Cai, D. P.; Xie, Z. X.; Zheng, L. S. Control of the Surface of ZnO Nanostructures by Selective Wet-Chemical Etching. *J. Phys. Chem. C* **2010**, *114*, 10114–10118.

51 Han, X. G.; Zhou, X.; Jiang, Y. Q.; Xie, Z. X. The Preparation of Spiral ZnO Nanostructures by Top-Down Wet-Chemical Etching and their Related Properties. *J. Mater. Chem.* **2012**, *22*, 10924–10928.

52 Han, X. G.; Jin, M. S.; Kuang, Q.; Xie, Z. Z. X.; Zheng, L. S. Directional Etching Formation of Single-Crystalline Branched Nanostructures: A Case of Six-Horn-like Manganese Oxide. *J. Phys. Chem. C* **2009**, *113*, 2867–2872.

53 Xie, S. F.; Han, X. G.; Kuang, Q.; Zhao, Y.; Xie, Z. X.; Zheng, L. S. Intense and wavelength-tunable photoluminescence from surface functionalized MgO nanocrystal clusters. *J. Mater. Chem.* **2011**, *21*, 7263–7268.